ARCHIVES
of
FOUNDRY ENGINEERING

ISSN (2299-2944)

10.24425/afe.2025.155353

Published quarterly as the organ of the Foundry Commission of the Polish Academy of Sciences

Scratch Test Studies on the Connection of Al_2O_3+40%TiO_2 Coating with AZ91 Alloy Casting

S. Olszewska *, M. Mróz
Rzeszow University of Technology, Poland
* Corresponding author. e-mail address: s.olszewska@prz.edu.pl

Received 09.01.25; accepted in revised form 16.04.25; available online 11.06.2025

Abstract

The paper presents the results of scratch tests on the connection of the Al2O3+40%TiO2 coating with the AZ91 alloy casting. The Al2O3+40%TiO2 coating was applied to the AZ91 alloy casting using the APS (Atmospheric Plasma Spraying) method. Microstructure studies and chemical composition analysis of the substrate material and the Al2O3+40%TiO2 coating were conducted. The analysis of the coating to substrate connection was based on microstructure examinations before and after the scratch test. The scratch was made in the direction from the substrate to the coating. In the scratch test, the depth and width of the scratch were determined. Based on the conducted research, it was found that the Al2O3+40%TiO2 coating has a very good quality connection with the AZ91 alloy substrate. The obtained lower values of the geometric parameters of the scratch (width and depth) for the Al2O3+40%TiO2 coating, compared to the AZ91 alloy substrate, indicate the potential use of the Al2O3+40%TiO2 coating to improve the scratch resistance of elements and machine parts made of the AZ91 alloy. The effect of the indenter's intervention during scratching is the degradation of the microstructure of the AZ91 alloy and the Al2O3+40%TiO2 coating. In this process, cracking plays the main role. In the case of the Al2O3+40%TiO2 coating, the effect of the indenter's action is a network of microcracks, while in the microstructure of the AZ91 alloy, cracks appeared in large precipitates of the γ-Mg17(Al, Zn)12 phase.

Keywords: AZ91 magnesium alloy, Al2O3+40%TiO2 coating, Scratch test

1. Introduction

Magnesium alloys are characterised by low density, high strength-to-weight ratio, good casting properties, and vibration damping capability. These advantages make magnesium alloys widely used in the aerospace, automotive, and electronics industries. Additionally, these alloys are easy to machine and recycle [1-5].

A significant limitation in the use of magnesium alloys is their susceptibility to corrosion, especially in humid environments and in the presence of aggressive ions, and their low abrasion wear resistance [6, 7].

One way to improve corrosion resistance and abrasion resistance is to use protective coatings. In the technical literature, there are studies on the use of conversion, electrolytic, laser, and plasma-sprayed coatings [7, 8].

The APS (Atmospheric Plasma Spraying) method can be used to apply metallic and ceramic coatings. The APS method involves melting or partially melting powder particles and accelerating them in a plasma stream, which solidify quickly upon contact with the substrate. The quality of the produced coatings is determined by the appropriate selection of APS process parameters, such as the type of plasma gas, the distance between the torch nozzle and the substrate, the torch movement speed, the amount of powder fed, its granulation, and others [9].

Among ceramic coatings, those based on aluminium oxide, particularly Al2O3+TiO2 coatings, are of great interest. These coatings, due to their high hardness and abrasive wear resistance, good corrosion resistance, and good adhesion to the substrate (in various configurations of titanium oxide TiO2 content), have a microstructure and operational properties that allow for a wide range of applications [10, 11].

The optimisation of APS process parameters for applying the Al2O3+40%TiO2 coating to stainless steel was studied by the authors of [12]. Their research focused on the analysis of microstructure, hardness, and abrasive wear resistance. They concluded that the technological parameters of the spraying process significantly affect the quality and adhesion of the coating to the substrate. Studies on the abrasion wear and corrosion resistance of aluminium oxide-based coatings were also conducted by the authors of [6, 13].

In turn, the authors of [14] used two variants of titanium oxide content (13% and 40%) to produce aluminium oxide-based coatings. The coatings were applied using the plasma spraying method onto an AZ31 alloy substrate. Based on their research, they observed a significant improvement in the tribological properties of AZ31 alloy samples with the coating.

A significant improvement in the corrosion resistance of the AZ31 alloy due to the application of the Al2O3+3%TiO2 coating was reported by the authors of [15]. Based on their study of resistance to 3.5% NaCl solution, they found that the Al2O3+3%TiO2 coating showed much better anticorrosive properties compared to the TiO2 coating.

A greater number of variants of titanium oxide content in the Al2O3-based coating were used by the authors of the study [16]. They analysed the microhardness and crack resistance of coatings containing 13%, 40%, and 50% TiO2. The coatings were applied to a substrate of AISI304L steel. The authors found that increasing the addition of titanium oxide results in a decrease in the microhardness of the coating.

In the technical literature, there are studies on the use of other methods for producing Al2O3+TiO2 coatings, such as HVOF [17], or flame spraying [18], as well as studies that examined Al2O3-based coatings with other additives, for example with chromium oxide [19] or aluminium [6].

This paper presents the results of the first stage of research on the use of Al2O3+40%TiO2 coating to improve the functional properties of the surface layer of AZ91 magnesium alloy castings. In the first stage, given that one of the main criteria for using this coating to improve the functional properties of the surface layer of AZ91 alloy castings is to achieve high-quality bonding of the coating to the substrate, the results of scratch resistance tests (scratch test) are presented. To identify cracks and delaminations, these test results were analysed based on microstructure studies and chemical composition analysis.

2. Materials and Research Methodology

The coating was applied to a substrate consisting of AZ91 magnesium alloy plates measuring 50x35x5 mm. The chemical composition of the material is presented in Table 1.

Table 1.
Chemical composition of AZ91 alloy

Element content, % wt.			
Al	**Zn**	**Mn**	**Mg**
8.75	0.49	0.22	rest

An example microstructure of the AZ91 alloy is shown in Figures 1 and 2.

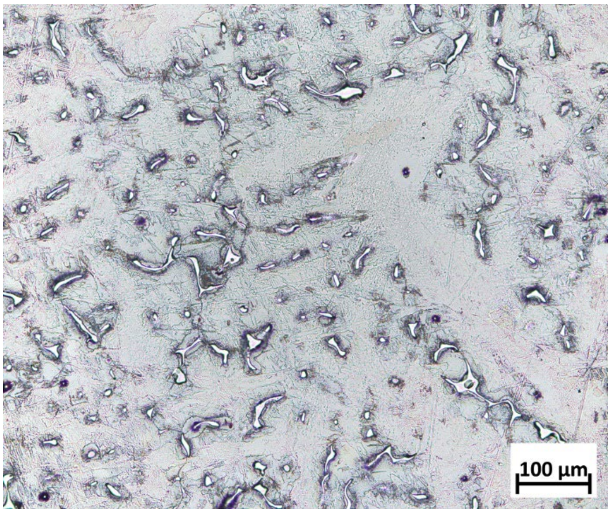

Fig. 1. Microstructure of AZ91 alloy, optical microscope, magnification 100x

The microstructure of the AZ91 alloy consists of a solid solution α, precipitates of the γ-Mg17(Al, Zn)12 intermetallic phase, and a β (α+γ) eutectic.

Before the coating application process, the substrate was subjected to abrasive blasting to increase the surface roughness. The samples were also cleaned with acetone.

The coating was made using Al2O3+40%TiO2 powder (60% Al2O3 and 40% TiO2). The appearance of the powder is shown in Figure 3. In the morphology of this powder, spherical particles with diameters ranging from 10 to 70 µm can be distinguished. Each spherical particle was a conglomerate of needle-like and globular microparticles (Fig. 4).

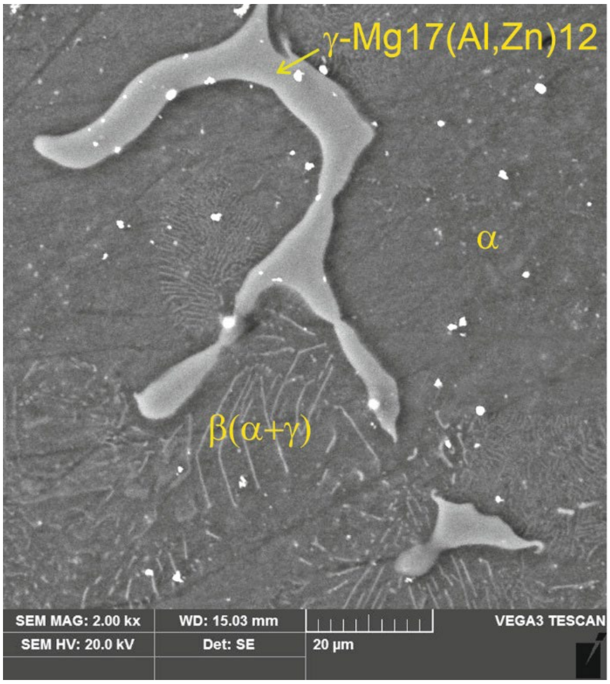

Fig. 2. Microstructure of the AZ91 alloy – SEM image

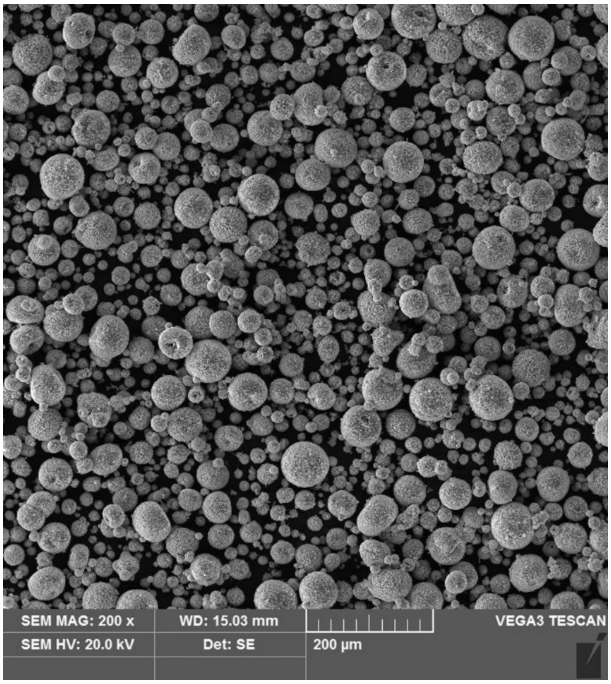

Fig. 3. Appearance of Al2O3+40%TiO2 powder particles

Based on the chemical composition analysis of the Al2O3+40%TiO2 powder particles, it was found that the needle-like microparticles (marked as 1) contain more titanium than the globular particles (marked as 2).

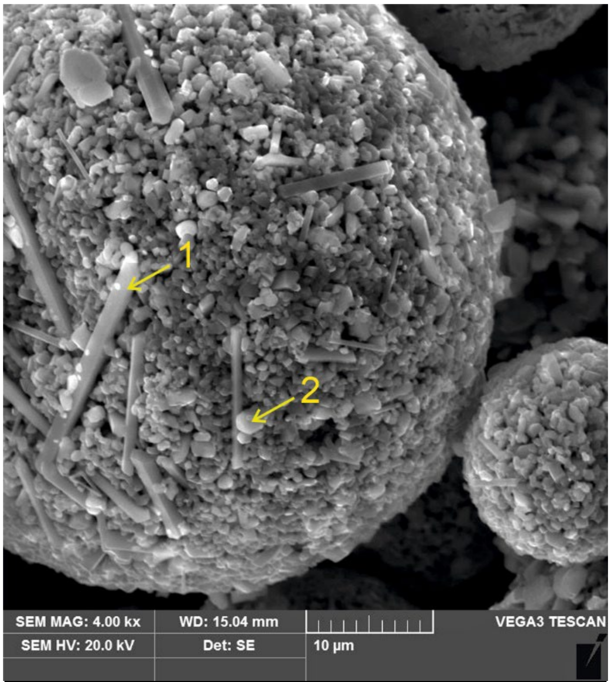

Point	Element, %wt.		
	O	Al	Ti
1	48.32	5.46	46.22
2	48.93	41.73	9.34

Fig. 4. Al2O3+40%TiO2 powder particle and results of its chemical composition analysis

The coating application process was carried out using a plasma spraying station with the APS method. Preliminary research results allowed for the determination of the technological parameters of the APS spraying process (Tab. 2). The criterion adopted was a coating thickness ranging from 280 to 300 µm.

Table 2.
Process parameters for spraying the Al2O3-TiO2 coating

Process parameter	Value
Amperage	600 A
Gas output	Ar – 55 l/min
	H – 10 l/min
Amount of powder fed	Dispenser disc – 0.45 rpm
	Mixer – 90%
Distance of the torch from the part to be sprayed	110 mm
Carrier gas for powder	Ar – 4 l/min
Type of refrigerant gas	Air, pressure 5 bar
Number of passes	20

A view of the AZ91 alloy sample with the Al2O3+40%TiO2 coating applied is shown in Figure 5.

Fig. 5. Al2O3+40%TiO2 coating

Microstructural studies and chemical composition analysis were conducted using a Tescan Vega 3 scanning microscope equipped with an Inca x-act X-ray microanalysis attachment.

Scratch resistance tests were performed using a Revetest device. The scratch length was 2 mm. The scratch was made in the direction from the substrate to the coating. The indenter load value was 5 N, with a scratch speed of 5 mm/min.

3. Research Results and Their Analysis

The microstructure of the Al2O3+40%TiO2 coating applied to the AZ91 alloy substrate is shown in Figure 6. Observation of the coating-substrate interface did not reveal any cracks or delaminations, indicating high-quality bonding of the coating to the substrate.

Figure 7 shows the results of the X-ray microanalysis of the Al2O3+40%TiO2 coating. Based on the obtained research results, it can be concluded that the layered structure of the coating contains areas with varying titanium content.

The results of the scratch test for the AZ91 alloy sample with the Al2O3+40%TiO2 coating are shown in Figure 8 and Table 3.

Table 3.
Scratch test results

Parameters	Material	
	AZ 91	**Coating Al2O3+40%TiO2**
Penetration depth, µm	4.0 – 8.2	2.1 – 2.9
Penetration width, µm	116.02 – 120.50	47.05 – 47.25
Friction Coefficient	0.2 – 0.28	0.1 – 0.3
Frictional force, N	0.75 – 1.3	0.45 – 1.6
Acoustic Emission, %	5.0 – 12.0	4.0 – 5.0

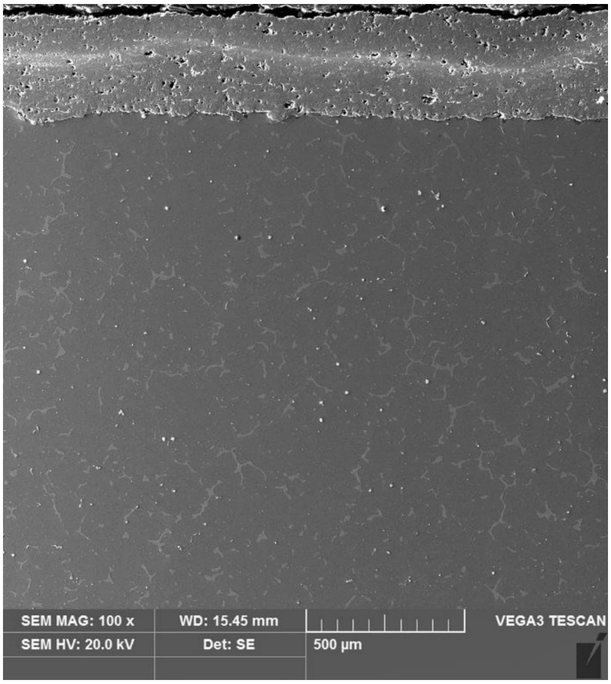

Fig. 6. View of the Al2O3+40%TiO2 coating's bonding with the AZ91 alloy substrate

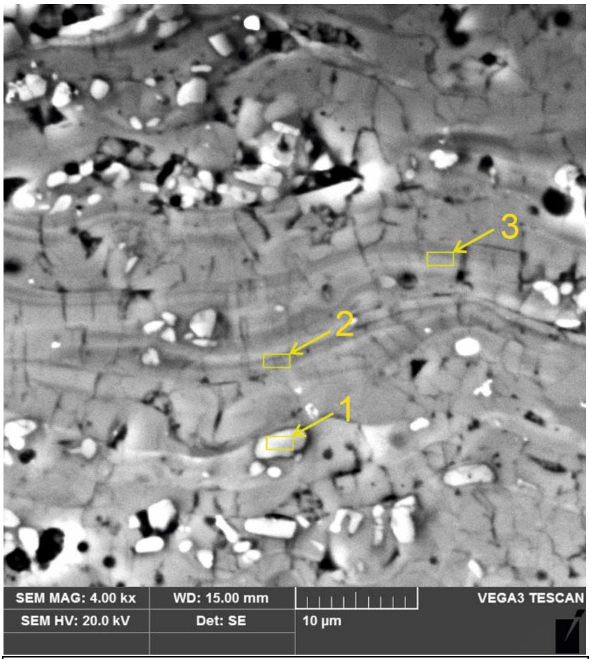

Area	Elemental content, %wt.		
	O	Al	Ti
1	51.98	45.66	2.36
2	48.43	31.24	20.33
3	47.71	30.21	22.08

Fig. 7. Microstructure of the Al2O3+40%TiO2 coating and results of the chemical composition analysis

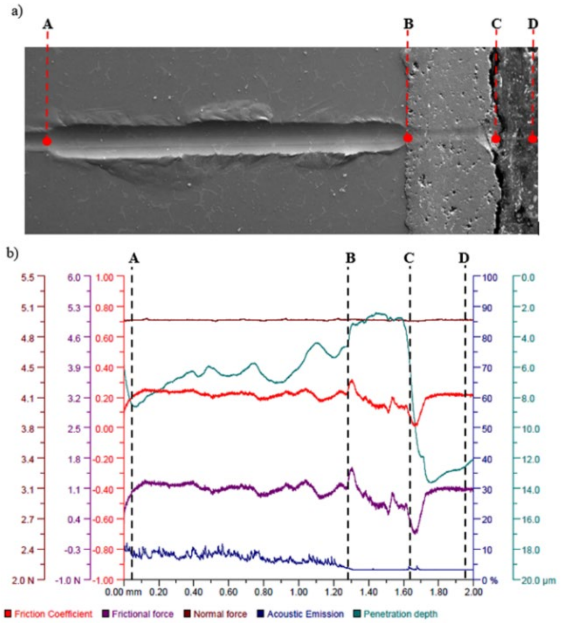

Fig. 8. View of the scratch surface (a) and scratch test results (b)

The scratch test results clearly show that the coating material is significantly more scratch-resistant than the AZ91 alloy. This is particularly evident in the scratch width. The width in the case of the coating is almost three times smaller compared to the scratch width in the AZ91 alloy (Fig. 9).

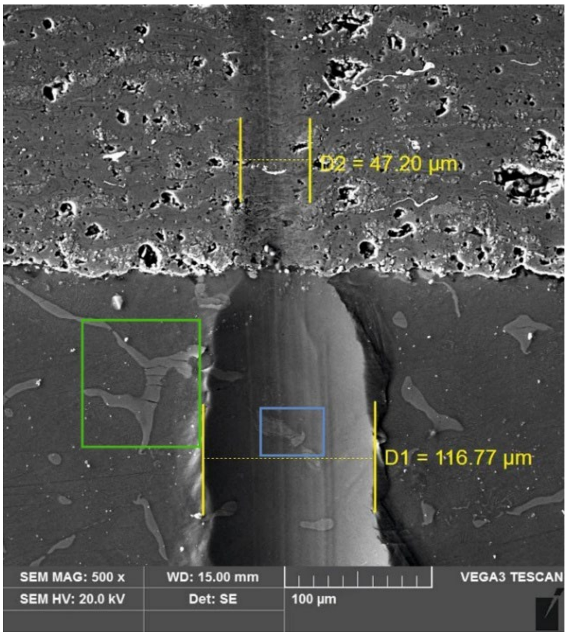

Fig. 9. View of the scratch in the Al_2O_3+40%TiO_2 coating and in the AZ91 alloy

The analysis of damage, cracks, and delaminations occurring at the substrate-coating transition boundary was conducted based on SEM images of this area (Fig. 10).

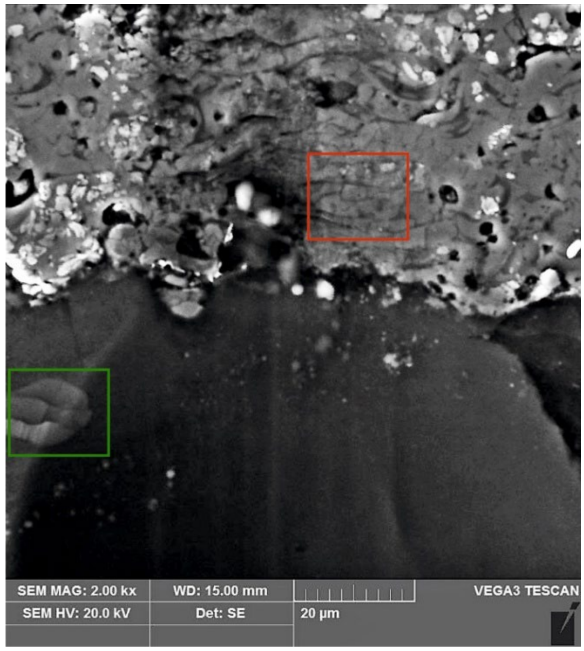

Fig. 10. View of the scratch at the substrate-coating transition boundary

Based on SEM image observations, no delaminations were found at the transition of the scratch from the AZ91 alloy substrate to the Al_2O_3+40%TiO_2 coating, indicating a high-quality bonding between the coating and the substrate. Observation of the scratch area in the coating behind the substrate showed the presence of a network of microcracks caused by the indenter's intrusion into its banded microstructure (marked in red in Fig. 10). Cracks were also found in the AZ91 alloy, where, due to the indenter's pressure, cracks appeared in large and thick precipitates of the intermetallic phase γ-$Mg_{17}(Al, Zn)_{12}$ (marked in blue in Fig. 9). The significant impact of the indenter on the AZ91 alloy microstructure is indicated by the presence of cracks in the large γ-$Mg_{17}(Al, Zn)_{12}$ phase precipitates, found not only in the scratch area but also nearby (marked in green in Figs. 9 and 10). The occurrence of these cracks during the scratch test is confirmed by the acoustic emission (AE) signal analysis results presented in Table 3 and Fig. 8. It can be assumed that the cracks in the γ-$Mg_{17}(Al, Zn)_{12}$ phase are due to its high hardness and brittleness.

4. Conclusions

Based on the conducted research, it was found that the Al_2O_3+40%TiO_2 coating has significantly higher scratch resistance compared to the AZ91 alloy.

The scratch test did not reveal the presence of delaminations and cracks at the scratch transition from the substrate to the coating, indicating a high-quality connection between the Al_2O_3+40%TiO_2 coating and the AZ91 alloy.

The effect of the indenter's intervention during scratching is the degradation of the microstructure of the AZ91 alloy and the Al2O3+40%TiO2 coating. In this process, cracking plays the main role. In the case of the Al2O3+40%TiO2 coating, the effect of the indenter's action is a network of microcracks, while in the microstructure of the AZ91 alloy, cracks appeared in large precipitates of the γ-Mg17(Al, Zn)12 phase. It can be assumed that these cracks were caused by the pressure of the plastic phase, which is the solid solution α, on the hard and brittle precipitates of the intermetallic phase γ-Mg17(Al, Zn)12.

Further research is planned to precisely explain the cracking mechanism of the γ-Mg17(Al, Zn)12 phase precipitates, including determining the critical size of these precipitates at which they start to crack. Therefore, in addition to the scratch test method, nanoindentation studies along with metallographic studies after deep etching are planned.

References

[1] Lai, L., Wu, H., Mao, G., Li, Z., Zhang, L. & Liu, Q. (2022). Microstructure and corrosion resistance of two-dimensional TiO_2/MoS_2 hydrophobic coating on AZ31B magnesium alloy. *Coatings*. 12(10), 1488, 1-12. DOI: 10.3390/coatings12101488.

[2] Xi, B., Fang, G. & Xu, S. (2018). Multiscale mechanical behavior and microstructure evolution of extruded magnesium alloy sheets: experimental and crystal plasticity analysis. *Materials Characterization*. 135, 115-123. DOI: 10.1016/j.matchar.2017.11.034.

[3] Yang, Y., Xiong, X., Chen, J., Peng, X., Chen, D. & Pan, F. (2021). Research advances in magnesium and magnesium alloys worldwide in 2020. *Journal of Magnesium and Alloys*. 9(3), 705-747. DOI: 10.1016/j.jma.2021.04.001.

[4] Wang G.G. & Weiler J.P. (2023). Recent developments in high pressure die-cast magnesium alloys for automotive and future applications. *Journal of Magnesium and Alloys*. 11(1), 78-87. DOI: doi.org/10.1016/j.jma.2022.10.001.

[5] Liu B., Yang J., Zhang X., Yang Q., Zhang J., & Li X. (2022). Development and application of magnesium alloy parts for automotive OEMs: A review. *Journal of Magnesium and Alloys*. 11(1), 15-47. DOI: 10.1016/j.jma.2022.12.015.

[6] Sun, H. & Ma, S. (2016). Microstructural characteristics and protection performances of plasma-sprayed Al_2O_3–Al composite coatings on AZ91D magnesium alloy. *Science and Engineering of Composite Materials*. 23(5), 467-474. DOI: 10.1515/secm-2014-0151.

[7] Xin, Y., Huo, K., Hu, T., Tang, G. & Chu, P.K. (2009). Mechanical properties of Al_2O_3/Al bi-layer coated AZ91 magnesium alloy. *Thin Solid Films*. 517(17), 5357-5360. DOI: 10.1016/j.tsf.2009.03.101.

[8] Chang, S.H., Niu, L., Su, Y., Wang, W., Tong, X. & Li, G. (2016). Effect of the pretreatment of silicone penetrant on the performance of the chromium-free chemfilm coated on AZ91D magnesium alloys. *Materials Chemistry and Physics*. 171, 312-317. DOI: doi.org/10.1016/j.matchemphys.2016.01.022.

[9] Liu, C., Liang, J., Zhou, J., Wang, L. & Li, Q. (2015). Effect of laser surface melting on microstructure and corrosion characteristics of AM60B magnesium alloy. *Applied Surface Science*. 343, 133-140. DOI: 10.1016/j.apsusc.2015.03.067.

[10] Basha, G.M.T., Srikanth, A. & Venkateshwarlu, B. (2020). A critical review on nano structured coatings for alumina-titania (Al_2O_3-TiO_2) deposited by air plasma spraying process (APS). *Materials Today: Proceedings*. 22(4), 1554-1562. DOI: doi.org/10.1016/j.matpr.2020.02.117.

[11] Michalak, M., Łatka, L., Sokołowski, P. & Ambroziak, A. (2019). Investigations of microstructure and selected mechanical properties of Al_2O_3+ 40 wt.% TiO_2 coatings deposited by Atmospheric Plasma Spraying (APS). *Welding Technology Review*. 91(8), 7-11. DOI: 10.26628/wtr.v91i8.1068.

[12] Ahmed, I. & Abdel Salam, H. (2011). Microstructure, corrosion, and fatigue properties of alumina-titania nanostructured coatings. *Journal of Surface Engineered Materials and Advanced Technology*. 1(3), 101-106. DOI: 10.4236/jsemat.2011.13015.

[13] Łatka, L., Niemiec, A., Michalak, M. & Sokołowski, P. (2019). Tribological properties of Al2O3+TiO2 coatings manufactured by plasma spraying. *Tribologia*. 283(1), 19-24. DOI: 10.5604/01.3001.0013.1431.

[14] Çelik, İ. (2016). Structure and surface properties of Al_2O_3–TiO_2 ceramic coated AZ31 magnesium alloy. *Ceramics International*. 42(12), 13659-13663. DOI: 10.1016/j.ceramint.2016.05.162.

[15] Bayram, T., Karabaş, M. & Kayalı, Y. (2023). Deposition and study of plasma sprayed Al_2O_3-TiO_2 coatings on AZ31 magnesium alloy. *European Mechanical Science*. 7(1), 35-40. DOI: 10.26701/ems.1175394.

[16] Yılmaz, R., Kurt, A.O., Demir, A. & Tatlı, Z. (2007). Effects of TiO2 on the mechanical properties of the Al_2O_3–TiO_2 plasma sprayed coating. *Journal of the European Ceramic Society*. 27(2-3), 1319-1323. DOI: 10.1016/j.jeurceramsoc.2006.04.099.

[17] Toma, F.L., Stahr, C.C., Berger, L.M., Saaro, S., Herrmann, M., Deska, D. & Michael, G. (2010). Corrosion resistance of APS-and HVOF-sprayed coatings in the Al_2O_3-TiO_2 system. *Journal of Thermal Spray Technology*. 19, 137-147. DOI: 10.1007/s11666-009-9422-2.

[18] Habib, K.A., Saura, J.J., Ferrer, C., Damra, M.S., Giménez, E. & Cabedo, L. (2006). Comparison of flame sprayed Al2O3/TiO2 coatings: Their microstructure, mechanical properties and tribology behavior. *Surface and Coatings Technology*. 201(3-4), 1436-1443. DOI: 10.1016/j.surfcoat.2006.02.011.

[19] Grimm, M., Conze, S., Berger, L.M., Paczkowski, G., Lindner, T. & Lampke, T. (2020). Microstructure and sliding wear resistance of plasma sprayed Al_2O_3-Cr_2O_3-TiO_2 ternary coatings from blends of single oxides. *Coatings*. 10(1), 42, 1-12. DOI: 10.3390/coatings10010042.